Comments on Inorganic Chemistry
Publication details, including instructions for authors and subscription information:
http://www.informaworld.com/smpp/title~content=t713455155

SCHIFF BASE MACROCYCLES: RELIABLE TEMPLATES FOR MULTINUCLEAR METALLOCAVITANDS

Peter D. Frischmann[a]; Mark J. MacLachlan[a]
[a] Department of Chemistry, University of British Columbia, Vancouver, BC, Canada

To cite this Article Frischmann, Peter D. and MacLachlan, Mark J.(2008) 'SCHIFF BASE MACROCYCLES: RELIABLE TEMPLATES FOR MULTINUCLEAR METALLOCAVITANDS', Comments on Inorganic Chemistry, 29: 1, 26 — 45
To link to this Article: DOI: 10.1080/02603590802026465
URL: http://dx.doi.org/10.1080/02603590802026465

Comments on Inorganic Chemistry, 29: 26–45, 2008

ISSN: 0260-3594 print
DOI: 10.1080/02603590802026465

Taylor & Francis
Taylor & Francis Group

SCHIFF BASE MACROCYCLES: RELIABLE TEMPLATES FOR MULTINUCLEAR METALLOCAVITANDS

PETER D. FRISCHMANN
MARK J. MacLACHLAN

Department of Chemistry, University of British Columbia, Vancouver, BC, Canada

Recent studies of polydentate Schiff base macrocycles indicate larger diameter macrocycles often deviate from planarity upon metal complexation, taking on a concave conformation. These bowl shaped complexes are reminiscent of organic cavitands, however, their dependence on metal coordination rather than C-C bonds for curvature has led us to dub them *metallocavitands*. In particular, we have prepared a family of soluble [3 + 3] Schiff base macrocycles from the condensation of 3,6-diformylcatechol with 1,2-dialkoxy-4,5-diaminobenzenes and investigated their ability to template the formation of metallocavitands. When reacted with seven equivalents of $Zn(OAc)_2$ or $Cd(OAc)_2$, hepta-nuclear metallocavitands are formed. Dimerization of these complexes into capsules has been observed and the thermodynamics of self-association has been studied. Tuning the cavity dimensions and strength of supramolecular self-association is easily achieved by switching metals. Isolation of a tetra-zinc intermediate has provided insight into the template effect our macrocycles exhibit. These results highlight the reliability of Schiff base macrocycles as scaffolds for metallocavitand formation.

***Keywords*: macrocycle, metal cluster, metallocavitand, Schiff base, supramolecular chemistry, template**

Address correspondence to Mark J. MacLachlan, Department of Chemistry, University British Columbia, 2036 Main Mall, Vancouver, BC V6T 1Z1, Canada. E-mail: mmaclach@chem.ubc.ca

INTRODUCTION

From fullerenes to resorcinarenes, molecules with curvature are aesthetically pleasing, useful, and ubiquitous throughout supramolecular chemistry.[1] One class of molecules that exemplifies the utility and beauty of molecular curvature is the cavitand. A term coined by Donald Cram,[2] *cavitand* refers to rigid, open bowl-shaped hosts that are capable of interacting in a complementary manner with smaller guest molecules. Calix[4]arenes, resorcin[4]arenes, and cyclotriveratrylenes are purely organic macrocycles that are also cavitands.

In solution, an intimate thermodynamic dance occurs between cavitand, guest, and bulk solvent. The volume, degree of curvature, and chemical environment of the cavity all play important roles in guest uptake making cavitands highly selective for guests based on their size and functional groups present. This parallel to enzymes makes cavitands excellent candidates for applications involving molecular recognition such as sensing,[3] metal separation,[4] host-guest catalysis,[5] and even molecular machinery.[6]

Despite nature's reliance upon the synergy of transition metal active sites and amino acid directing groups for molecular recognition, transition metals are mostly absent from synthetic cavitands. The examples of metal-containing cavitands that do exist show interesting molecular recognition properties and are typically monometallic, where the metal is found either at the periphery or in the bottom of the cavity.[7] In these systems, the metal is coordinated to a preformed organic cavity and has little impact on the intrinsic bowl-shape of the parent cavitand. Cavitands with multiple metals introduced into the cavity could mimic more complex metalloenzymes and provide a wealth of novel molecular recognition applications. Literature examples of *metallocavitands*, multimetallic complexes where metal coordination is necessary for cavity formation, are rare and often isolated by accident.[8]

The lack of a paradigm for the synthesis of metallocavitands has kept them from the mainstream attention that their organic counterparts have received. This is most likely due to the often unpredictable bonding between metals and ligands relative to tetravalent carbon-carbon bonds. The design of rigid ligands that consistently form multi-metallic complexes possessing significant molecular curvature would greatly accelerate scientists' adoption of metallocavitands as useful supramolecular tools. Recent studies of Schiff base macrocycles suggest that these compounds may fill this void.

MOLECULAR CURVATURE IN MULTI-METALLIC SCHIFF BASE MACROCYCLES

Since Robson's inaugural [2+2] macrocycle,[9] **1** (Chart 1),[10] Schiff base macrocycles have proven useful as substrates in the study of metal-metal interactions. In general, these macrocycles are easily synthesized by reacting a diamine monomer with a diformyl monomer of appropriate geometry, yielding a single macrocycle as the thermodynamic product. Families of macrocycles may be developed through the facile functionalization of individual monomers prior to cyclization. The polydentate nature of Schiff base macrocycles, especially those macrocycles possessing multiple phenoxy groups, facilitates the formation of multi-metallic complexes. Although many macrocycles are planar, recent studies involving larger diameter Schiff base macrocycle complexes reveal their tendency to adopt concave or saddle-like geometries similar to traditional organic cavitands.

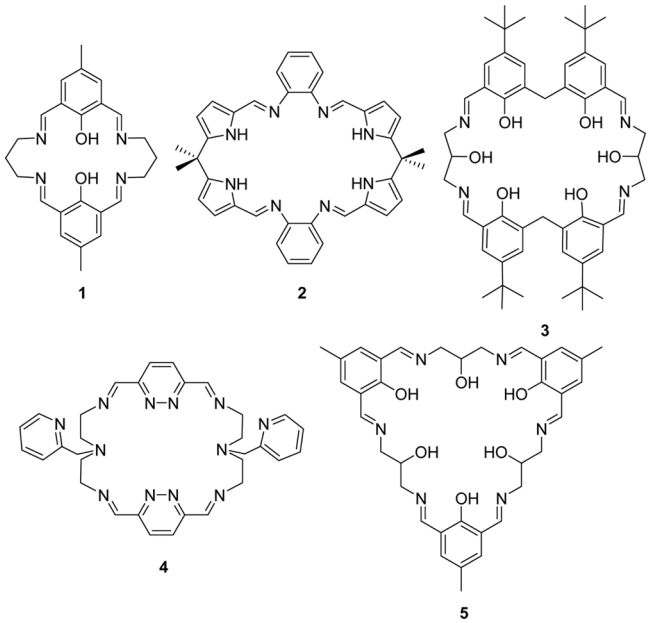

Chart 1. Schiff base macrocycles that coordinate to multiple metal ions and exhibit concave structures.

One emerging family of macrocycles that exhibit molecular curvature are the [2+2] Schiff base calix[4]pyrrole macrocycles, **2**, developed by Love and coworkers as well as Sessler and coworkers.[11] Generally bimetallic, the curvature of these macrocycle metal complexes is a saddle shape similar to the Pac-Man porphyrin complexes. The dicobalt-containing macrocycle is capable of dioxygen reduction,[12] whereas the dizinc and dicadmium complexes abstract fluoride from BF_4^-.[13]

Reminiscent of a calixarene, the [2+2] Schiff base macrocycle **3**, reported by McKee and coworkers, is capable of forming bi-, tri-, or tetrametallic complexes with a variety of metals.[14] Upon coordination of two zinc, nickel, or cobalt ions, the macrocycle adopts a bowl shape that fits our definition of a metallocavitand.[15] Similar bimetallic metallocavitands have been isolated by Weitzer and Brooker from the pyridazine-containing Schiff base macrocycle, **4**.[16]

The [3 + 3] macrocycle **5** was metal-templated by Thompson and coworkers and the solid-state structure revealed a dumbbell-shaped, dodecacopper dimacrocycle complex.[17] Each macrocycle exhibits a metallocavitand-like concave curvature where the cavity points away from the cluster. The reliability of macrocycle **5** to form multi-metallic complexes exhibiting molecular curvature was emphasized by the isolation of a tetradecacopper dimacrocycle complex.[18] In this solid-state structure, the metal cluster occupies the cavity of each macrocycle.

The tendency of Schiff base macrocycle complexes to deviate from planarity as their size increases from the original [2+2] Robson type macrocycle is illustrated by these examples. To date, researchers have focused their efforts primarily on structural studies and the catalytic and magnetic properties that arise due to the proximity of multiple metals coordinated inside the macrocycles. The predisposition towards cavity formation has been mostly overlooked despite the vast potential for molecular recognition applications. This has led us to seek large, polydentate, Schiff base macrocycles that will consistently adopt a rigid bowl shape induced by metal coordination, the essence of a metallocavitand.

TRIS-SALPHEN [3+3] SCHIFF BASE MACROCYCLE

Given the rich and versatile coordination chemistry of salphens (N,N-bis-salicylidenephenylenediamine), we set out (in 2001) to develop a shape-persistent macrocycle that possesses three salphen-like units as well as a central, crown ether-like interior (Scheme 1, **6a–e**). Previously,

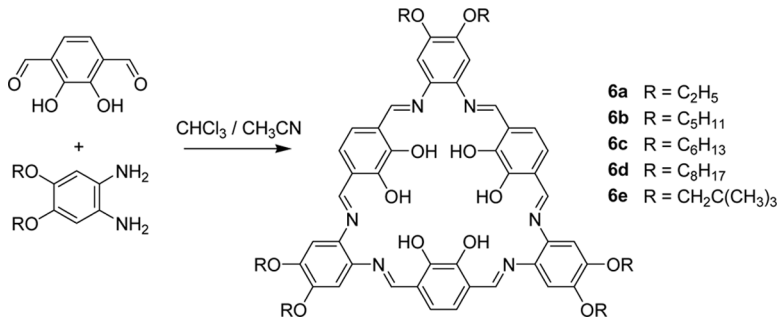

Scheme 1. Synthesis of tris-salphen macrocycles **6a–e**.

Reinhoudt and coworkers reported macrocycles with similar construction based on naphthalenedialdehydes, but they found that these products were insoluble and required a Ba^{2+} template.[19] While we were pursuing soluble macrocycles **6a–e**, the analogue with no alkoxy substituents was isolated and characterized.[20] Soluble macrocycles **6a–e** are synthesized by reacting the geometrically programmed 3,6-diformylcatechol with 1,2-dialkoxy-4,5-diaminobenzenes in refluxing $CHCl_3/CH_3CN$ as depicted in Scheme 1.[21] The [3+3] cyclization proceeds in a matter of hours with no observation of larger/smaller cyclized products. Upon cooling to room temperature, the macrocycles are isolated by filtration in yields of ca. 80% with no further purification necessary. Solubility is easily tuned by altering the peripheral alkoxy chains on the diamine monomer.

As expected, one phenoxy, one imine, two aromatic, and one OCH_2 resonances are observed in the ^1H NMR spectra of macrocycles **6a–e** indicating the presence of C_3 rotational symmetry. The triplet splitting pattern observed for the OCH_2 resonance in macrocycles **6a–d** and singlet for **6e** are indicative of a horizontal mirror plane confirming their assignment to the D_{3h} point group in solution, although calculations reveal that the lowest energy conformation is non-planar.[21] A large downfield shift to ca. 13–16 ppm is observed for the phenoxy resonance, a sign of the strong intramolecular hydrogen bonding. The molecular ion, sodium adduct, and oligomeric tubular aggregates[22] are observed for each macrocycle by electrospray ionization mass spectrometry (ESI-MS) and matrix assisted laser desorption ionization time of flight mass spectrometry (MALDI-TOF MS). A single-crystal X-ray

diffraction (SCXRD) study of macrocycle **6a** revealed a non-planar conformation where one catechol unit is slightly above the plane of the macrocycle, one is slightly below, and the other is nearly coplanar with the three phenylenediimines in the macrocycle.

HEPTA-ZINC METALLOCAVITANDS

Macrocycles **6a–e** template the formation of hepta-zinc acetate clusters in their interior when reacted with 7 equivalents of $Zn(OAc)_2$, yielding metallocavitands **7a–e**, as shown in Scheme 2.[23] Metallation of the salphen pockets was evident from the loss of phenoxy resonances in the ^1H NMR spectra. C_3 rotational symmetry is still present but the complex coupling pattern observed for the OCH_2 resonance of complexes **7a–d**, simulated as an ABX_2 spin system, and the doublet observed for **7e**, are evidence for the loss of the parent macrocycle's horizontal mirror plane. Two methyl resonances assigned to acetate ligands were also observed in the ^1H NMR spectra. In most cases the molecular ion as well as tetra-, penta-, and hexa-zinc fragments were observed in the ESI and MALDI-TOF mass spectra. The structure of metallocavitands **7a–e** could not be confirmed without SCXRD experiments.

Our first glimpse of the bowl geometry came when single crystals of **7a**, grown from DMSO/ether, were subjected to a SCXRD experiment. Figure 1 depicts the solid state structure of **7a**. The label scheme found in

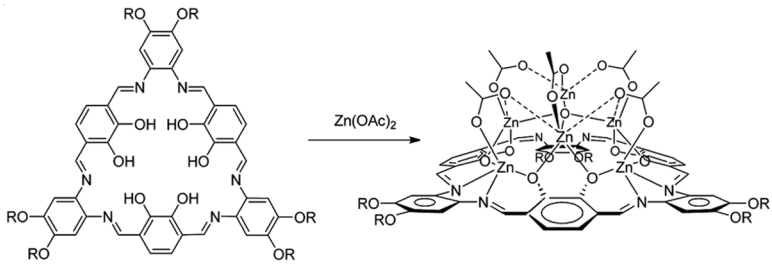

Scheme 2. Synthesis of hepta-zinc metallocavitands **7a–e** from macrocycles **6a–e**. The seventh zinc ion and sixth acetate ligand are obscured by the cluster. Reprinted with permission from Ref. 25. Copyright 2008 American Chemical Society.

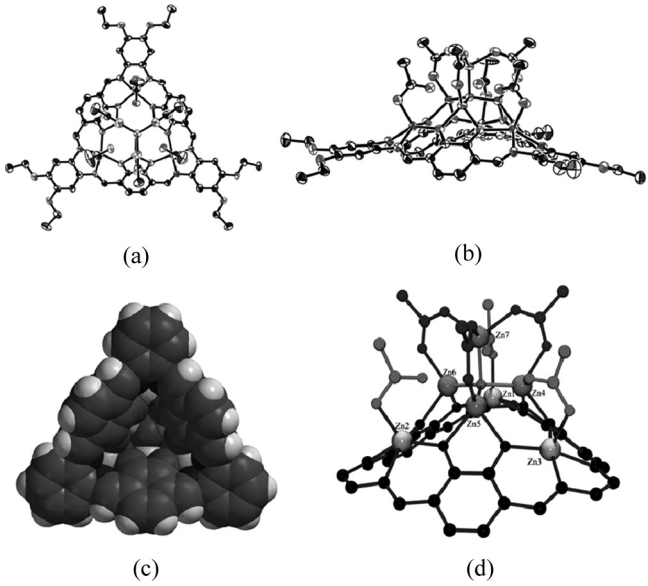

Figure 1. Solid-state structure of **7a**. a) Top down. b) Side on. c) Space filling depiction looking into the cavity. d) Magnified view of the Zn_7 cluster. The peripheral alkoxy groups have been omitted from figures c) and d). For the ORTEPs in a) and b), all ellipsoids are at 50% probability.

Figure 1d will be used to describe the metallocavitand. The three N_2O_2 pockets are occupied by zinc ions 1–3 (square pyramidal geometry). The fifth coordination site of Zn^{1-3} is filled by an acetate ligand bound to the apical position. Atop the trimetallated macrocycle is a distorted tetrahedral Zn_4O cluster. The acetate ligands coordinate in a μ-1,1,2 fashion, fastening the Zn_4O cluster to the macrocycle through Zn^{1-3}. Zinc ions 4–6 (distorted octahedral) make up the base of the Zn_4O tetrahedron and are bound to a bidentate catechol unit, two tridentate acetates, one bidentate acetate, and a central μ_4-oxo ligand. The acetate ligands in stabilize the Zn_4O cluster by bridging Zn^{4-6} to Zn^7 (tetrahedral) in a bidentate fashion. We were surprised by the macrocycle's significant deviation from planarity and the high nuclearity of the zinc acetate cluster.

Nearly identical structures were observed from SCXRD experiments of metallocavitands **7b** and **7e** providing evidence of a strong template effect exhibited by macrocycles **6a–e** for formation of the hepta-zinc cluster. Peripheral alkyl groups appear to have no effect on the observed

solid-state coordination geometry but do alter the intermolecular crystal packing. Following our report of these complexes, the analogue with butyloxy substituents was also structurally characterized.[24] The robust template effect of the macrocycles has also been demonstrated with other carboxylates such as zinc methacrylate[25] and zinc n-propionate.[24] Each carboxylate yielded an analogous hepta-zinc metallocavitand confirmed by standard spectroscopic techniques.

EVIDENCE FOR HEPTA-ZINC CLUSTER TEMPLATION

Upon close examination of the tetrahedral Zn_4O cluster that caps metallocavitands **7a–e**, a significant resemblance to basic zinc acetate (BZA),[26] a tetrahedral $Zn_4O(OAc)_6$ cluster, becomes apparent. Figure 2 depicts the cluster of **7e** and BZA for comparison. This similarity encouraged us to qualitatively investigate the mechanism of formation for metallocavitands **7a–e**.

The two simplest explanations for this cluster formation are (a) BZA forms in solution and coordinates to the trimetallated macrocycle, or (b) the macrocycle *templates* the cluster coordination in a stepwise fashion. Both explanations are represented graphically in Figure 3. Note that from mass spectrometry we have evidence that the first three zinc ions occupy the N_2O_2 pockets, so this is a logical starting point.[23] We hypothesized that the macrocycle template mechanism, (b), is most probable since the reported synthesis of BZA involves heating zinc acetate under vacuum resulting in the loss of acetic anhydride, but

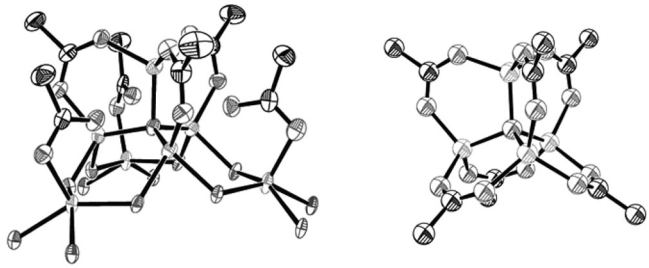

Figure 2. Solid state comparison of: a) the distorted tetrahedral Zn_4O cluster found on metallocavitand **7e**; b) perfectly tetrahedral basic zinc acetate (BZA). The central tetrahedral oxo ligand is bound to four zinc ions in both structures. Reprinted with permission from Ref. 25. Copyright 2008 American Chemical Society.

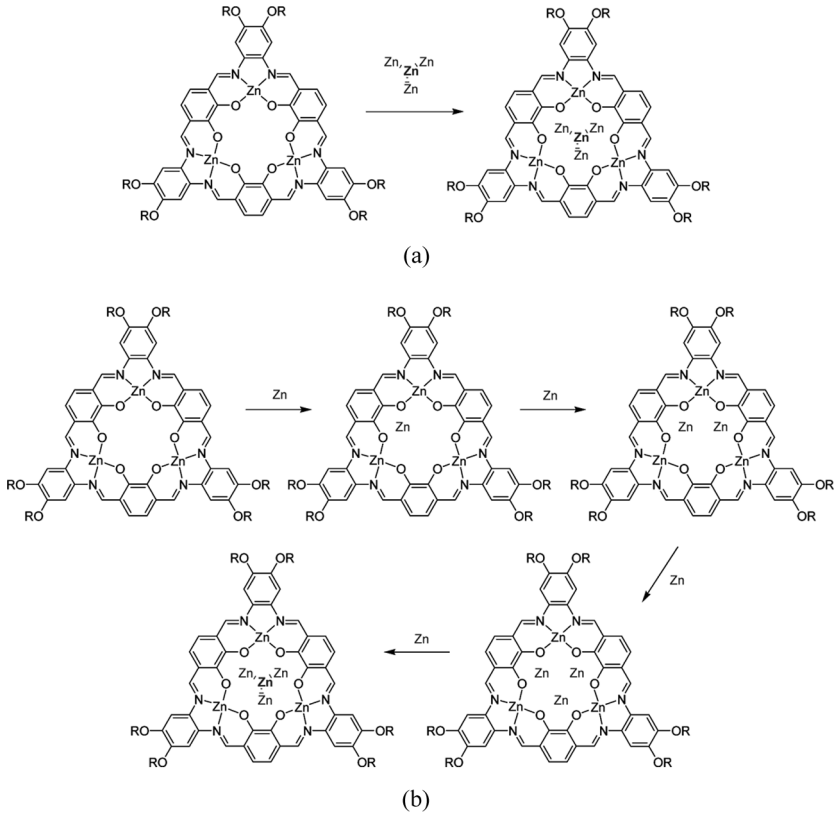

Figure 3. Two proposed mechanisms of Zn_4O cluster formation inside macrocycles **6a–e**: a) BZA forms in solution and coordinates to the trimetallated macrocycle; b) the trimetallated macrocycle templates the Zn_4O cluster in its interior. All acetate and oxo ligands have been omitted (all zinc atoms are Zn^{2+}).

complexes **7a–e** may be synthesized at room temperature and pressure in EtOH.

To investigate the macrocyclic template hypothesis, we reacted macrocycle **6e** with 4 equivalents of zinc acetate in EtOH. Tetra-zinc complex, **8**, was isolated as an orange solid and subjected to spectroscopic analysis.[25] Observation of three imine, six aromatic, and no phenoxy resonances in the ^{1}H NMR spectrum supported a C_s symmetric structure. Confirmation of the C_s symmetry observed in solution was provided by a SCXRD experiment conducted on crystals of **8** grown from a DMF/pyridine solution. The structure is depicted in Figure 4.

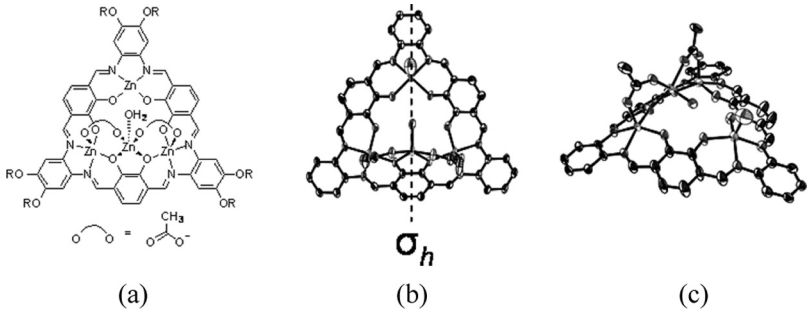

Figure 4. a) Pictorial representation of tetra-zinc complex **8** (R = $CH_2C(CH_3)_3$). b) Top down ORTEP depiction of **8** and the mirror plane. c) Side on view of **8** highlighting the central aqua ligand poised to become the μ_4-O of metallocavitand **7e**. The peripheral neopentyloxy chains have been omitted and all ORTEPs are at 50% probability.

As anticipated, each N_2O_2 pocket is coordinated to a zinc ion that exhibits square pyramidal geometry. The fourth zinc ion is found above the plane of the macrocycle, with its square pyramidal coordination sphere occupied by one catechol unit, two acetate ligands, and an aqua ligand. The aqua ligand is centrally located and perfectly poised to become the central μ_4-oxo ligand found in the parent hepta-zinc complex **7e**. Of the three zinc ions found in N_2O_2 pockets, two are coordinated to an acetate ligand and the third is coordinated to an aqua ligand in the apical positions. Another tetra-zinc intermediate with bridging methacrylate ligands has been isolated and crystallographically characterized.

To further demonstrate that complex **8** is an intermediate en route to the hepta-zinc metallocavitand **7e**, we conducted a ^{1}H NMR titration experiment, which is shown in Figure 5. $Zn(OAc)_2$ was added in 0.5 molar equivalents (Zn^{2+}:**6e**) to a solution of tetra-zinc complex **8**, dissolved in DMF-d_7, and spectra were recorded after each addition. Resonances corresponding to **7e** began to emerge after 5.5 equiv of $Zn(OAc)_2$ were added and finally dominated the spectrum after 7.0 equiv had been added. The complete conversion of **8** to **7e** upon addition of 3.0 equiv of $Zn(OAc)_2$ confirms that **8** is an isolable intermediate in the formation of hepta-zinc metallocavitand **7e**. Attempts to isolate penta- and hexa-zinc intermediates were unsuccessful.

Tetra-zinc intermediate **8** has potential to form mixed-metal clusters, which may be of interest as metalloenzyme mimics as well as magnetic materials. To probe this potential, **8** was reacted with 4 equiv of

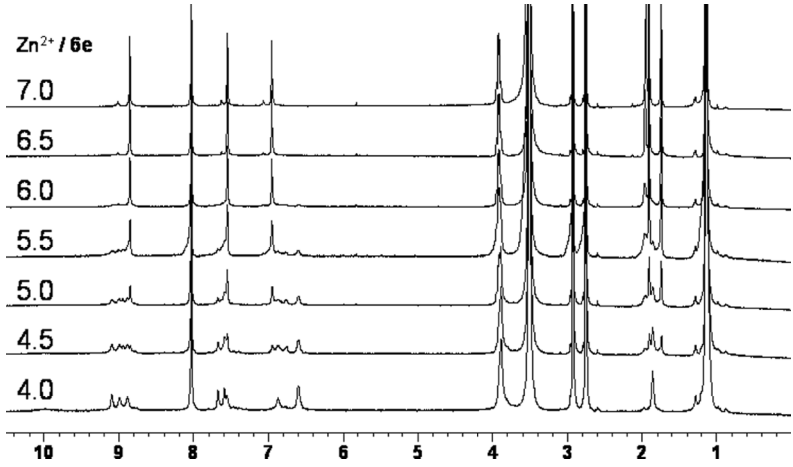

Figure 5. The conversion of tetra-zinc intermediate **8** to hepta-zinc metallocavitand **7e** was monitored by ^{1}H NMR spectroscopy in DMF-d_7. A solution of $Zn(OAc)_2$ was titrated into a solution of **8** in 0.5 molar equivalents. The ratio of Zn^{2+} to macrocycle **6e** is denoted on the left of each spectrum. Conversion from C_s symmetry to C_3 rotational symmetry is observed in the imine, aromatic, and acetate resonances.

$Co(OAc)_2$ in refluxing EtOH. Cobalt was chosen because tetrahedral Co_4O clusters similar to BZA are known.[27] A MALDI-TOF mass spectrum of the reaction mixture revealed overlapping isotopic distributions for the mixed-metal clusters $[(\mathbf{6e}\text{-}6H)Zn_4Co_3O(OAc)_5]^+$ and $[(\mathbf{6e}\text{-}6H)Zn_3Co_4(OAc)_5]^+$. The isotopic distribution of cluster $[(\mathbf{6e}\text{-}6H)Zn_3Co_3(OAc)_3]^+$ perfectly matched the calculated distribution, confirming the formation of a mixed metal cluster. This $[(\mathbf{6e}\text{-}6H)Zn_3Co_3(OAc)_3]^+$ signal is most likely due to fragmentation of larger heptanuclear clusters. We speculate that the heptanuclear, mixed-metal clusters have similar geometry to the hepta-zinc metallocavitands, but we have not yet structurally characterized one.

HEPTA-CADMIUM METALLOCAVITANDS

Generally, the cavities of organic cavitands have fixed dimensions that require a number of premeditative additional synthetic steps to alter. The ability to tune cavity dimensions of a bowl-shaped molecule in a single step is highly desirable. The cavities of our metallocavitands are easily tuned by switching metal ions. Since coordination of the N_2O_2 pockets of **6a–e** by Zn^{2+} resulted in a large deviation from planarity in

the parent macrocycle, we anticipated an even greater puckering effect when the larger Cd^{2+} ion is coordinated.

The reaction of **6d** with seven equivalents of $Cd(OAc)_2$ in EtOH yielded hepta-cadmium complex, **9d**, as an orange powder that was easily isolated by filtration (Scheme 3).[28] ^1H NMR spectroscopy revealed a product with C_3 rotational symmetry and a complex coupling pattern for the OCH_2 resonance simulated by an ABX_2 spin system, analogous to **7d**. Cadmium satellites with $^3J_{Cd\text{-}H} = 34.2$ Hz were observed for the imine resonance, confirming coordination of the N_2O_2 pockets. Similar results were observed when reacting **6a** and **6e** with seven equivalents of $Cd(OAc)_2$.

A SCXRD experiment on crystals of **9a**, grown from DMF, revealed the solid-state structure to be a hepta-cadmium metallocavitand as shown in Figure 6. Although similar to its hepta-zinc cousin, **7a**, there are some distinct differences. Each cadmium ion in the N_2O_2 pockets is in a distorted pentagonal pyramidal geometry with the capping acetate ligand filling the final two coordination sites in a bidentate manner. These acetate ligands bind in an unusual μ-1,1,1,2 fashion between three cadmium ions. The capping Cd_4O cluster consists of a trigonal pyramidal $Cd_3(\mu_3\text{-}O)$ cluster (pentagonal bipyramidal Cd^{2+} ions) bridged to a $[Cd(H_2O)_3]^{2+}$ ion (octahedral) by three μ-1,1,2 tridentate acetate ligands. The larger radius of Cd^{2+} vs. Zn^{2+} ions indeed puckered the macrocycle into an even more concave geometry and forced the capping Cd_4O cluster out of tetrahedral geometry. Surprisingly, metallocavitand **9a** is stable in boiling water for hours.

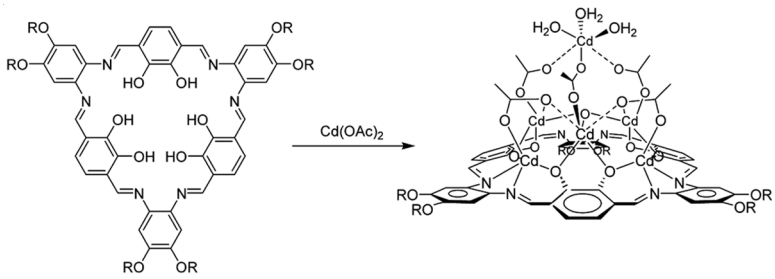

6a R = C_2H_5
6d R = C_8H_{17}
6e R = $CH_2C(CH_3)_3$

9a R = C_2H_5
9d R = C_8H_{17}
9e R = $CH_2C(CH_3)_3$

Scheme 3. Synthesis of hepta-cadmium metallocavitands. The seventh cadmium ion and sixth acetate ligand are obscured by the metal oxo cluster. Reproduced from Ref. 28 by permission of the Royal Society of Chemistry.

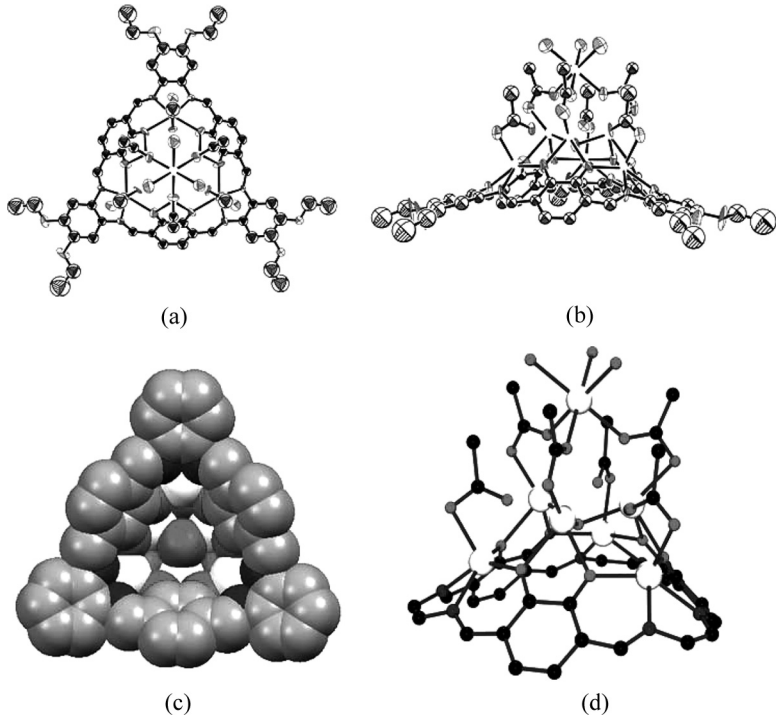

Figure 6. Solid-state structure of hepta-cadmium metallocavitand **9a**. a) Top down ORTEP. b) Side on ORTEP. c) Space filling view of the cavity. d) Magnified view of the Cd_7 cluster. The peripheral alkoxy groups have been omitted from figures c) and d). For the ORTEPs in a) and b), all ellipsoids are at 50% probability.

Interlocking dimers of **9a** exist in the solid state with one metallocavitand rotated 60° from the other on an axis that passes through the cavity and Cd_7 cluster of each metallocavitand. The capsule has crystallographic D_{3d} symmetry in the solid state and is shown in Figure 7. Electron density corresponding to a single DMF molecule was found inside the capsule but the guest appeared to be disordered between twelve equivalent orientations prohibiting its modeling. This promising result encouraged us to undertake solution-based dimerization studies.

METALLOCAVITAND CAPSULES

Dynamic exchange became evident when broad imine and aromatic resonances were observed in the ^{1}H NMR spectrum of **9a** in DMF-d_7 at

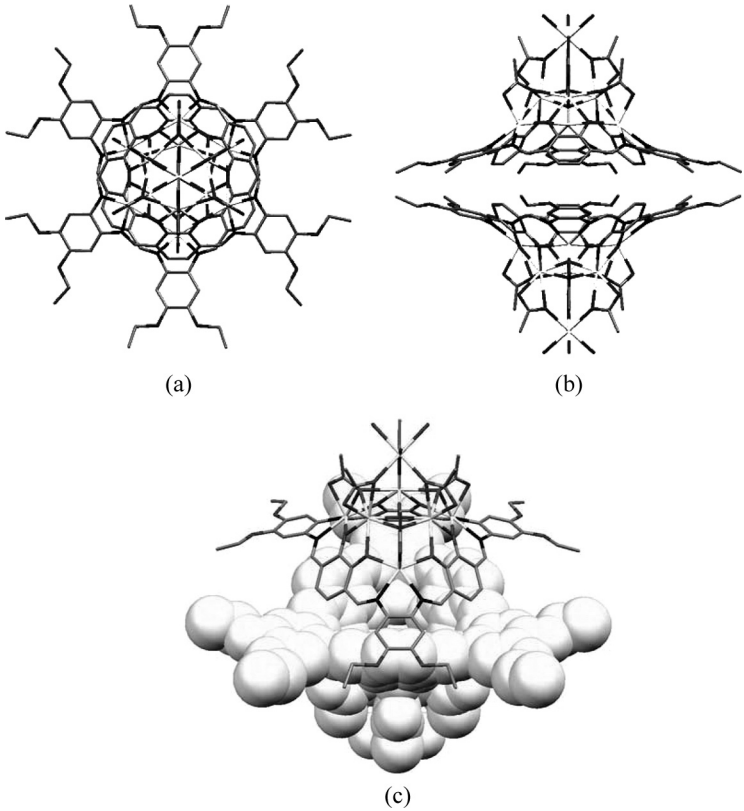

Figure 7. Solid-state capsules of metallocavitand **9a**. a) Top down view. b) Side on view. c) Space filling view of the cavity.

room temperature. When the sample was chilled, the aromatic and imine peaks broadened significantly more and eventually separated into two resonances as shown in Figure 8. Upon heating, the resonances coalesced and sharpened, giving the expected spectrum for a species exhibiting C_3 rotational symmetry. Cadmium satellites could eventually be observed above 311 K on the imine resonance.

At low temperature, the relative intensities of the aromatic resonances varied with concentration, allowing us to assign resonances to monomer and dimer. Shielding of 0.8 ppm was observed for proton H_c upon dimerization, consistent with the formation of a face-to-face capsule where H_c' is directly above the π cloud of the opposing catechol

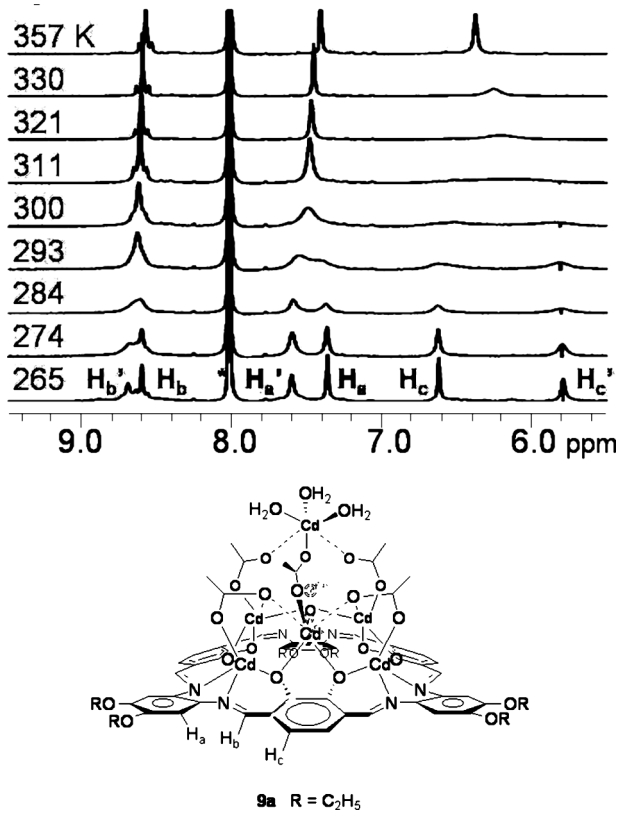

Figure 8. Dimerization of metallocavitand **9a** in DMF-d_7 probed by variable temperature ^{1}H NMR spectrosopy. Protons are labeled according to the structure on the bottom. Primes denote resonances assigned to dimers of **9a** ([**9a**] = 5 mmol L^{-1}). Reproduced from Ref. 28 by permission of the Royal Society of Chemistry.

ring. A van't Hoff plot was made from association constants calculated by integration of the aromatic protons at 238, 247, 256, and 265 K. In DMF-d_7, the K_{dim} (25°C) = 270 ± 10 L mol^{-1}, $\Delta H = 19 \pm 1$ kJ mol^{-1}, and $\Delta S = 110 \pm 2$ J mol^{-1} K^{-1}. These results indicate dimerization of **9a** is an entropy driven and enthalpy opposed process.

Investigation of this supramolecular dimerization in other solvents was performed using metallocavitand **9d** with peripheral octyloxy substituents to enhance solubility. Sharp resonances were observed in the ^{1}H NMR spectrum of **9d** in $CDCl_3$; in benzene-d_6, toluene-d_8, and

p-xylene-d_{10}, however, significant broadening of resonances was evidence for dimerization. Rapid exchange, even at low temperature, prevented observation of distinct monomer and dimer resonances in these solvents but the imine chemical shift varied with temperature and concentration. The variation in imine chemical shift was monitored in variable temperature, variable concentration ^{1}H NMR experiments (VTVC) and fit well to a model for dimerization allowing thermodynamic parameters of dimerization to be determined.[29] Thermodynamic data is summarized in Table 1.

For comparison, thermodynamics of dimerization for hepta-zinc metallocavitand **7d** were studied in benzene-d_6 by VTVC ^{1}H NMR spectroscopy. Surprisingly, at 25°C, the association constant for **7d** is 10 ± 3 L mol^{-1}, nearly two orders of magnitude lower than that of **9d**. The enthalpic differences are most noticeable between the two, possibly explaining the large deviance in K_{dim}. By simply switching metals, we can influence the geometry of the cavities and greatly alter the dimerization process.

Drawing from the pioneering work of Cram and Rebek,[30] the trend of entropy driven dimerization may be attributed to the expulsion of solvent from the monomer's cavity upon dimerization. This phenomenon is similar to the hydrophobic effect but rarely occurs in non-polar, organic solvents. Aromatic solvent molecules interact in a π-π fashion inside the cavity of metallocavitands **9d** and **7d**. When dimerization occurs, the solvent is expelled, increasing the entropy of the system.

No clear trends exist for the enthalpy of dimerization. This may be the result of a delicate balance between metallocavitand-solvent, metallocavitand-metallocavitand, and solvent-solvent interactions.

Table 1. Thermodynamic parameters for dimerization of hepta-cadmium metallocavitands **9a** (R = C_2H_5) and **9d** (R = C_8H_{17}) compared to hepta-zinc metallocavitand **7d** (R = C_8H_{17})

Complex	Solvent	K_a (25°C) - L mol^{-1}	ΔH - kJ mol^{-1}	ΔS - J mol^{-1} K^{-1}
9a	DMF-d_7	270 ± 10	19 ± 1	110 ± 2
9d	benzene-d_6	800 ± 100	-7 ± 5	32 ± 14
	toluene-d_8	1500 ± 400	1 ± 4	64 ± 14
	p-xylene-d_{10}	1000 ± 300	11 ± 8	94 ± 24
7d	benzene-d_6	10 ± 3	24 ± 12	100 ± 34

Host-guest studies involving complexes **9a, 9d**, and **7d** are alluring. There is great potential for unique catalysis, molecular recognition, and sensing inside of cavities constructed of multimetallic clusters. Metals bound to the periphery of organic cavitands have interacted in unusual ways with encapsulated guests.[7d] To date, the fast exchange of metallocavitands **9d** and **7d** in solvents that facilitate dimerization has made host-guest studies difficult. Although distinct resonances for monomer and dimer may be resolved for metallocavitand **9a** in DMF-d_7, the abundance and quality of DMF as a guest has so far prevented observation of significant binding to other guests.

CONCLUSIONS

We have demonstrated that the [3+3] Schiff base macrocycle with three salphen pockets is an excellent template for the formation of metallocavitands. Both hepta-zinc and hepta-cadmium cluster metallocavitands have been isolated and characterized by a variety of techniques in solution and the solid state. By switching between cadmium and zinc, the cavity dimensions are easily tuned, dramatically impacting the strength of self-assembly. These results demonstrate the template effect of the macrocycle and the tendency of large Schiff base macrocycle complexes to deviate from planarity. Capsule formation has been observed for both systems in a variety of solvents. This entropy-driven process is a result of solvent expulsion from the cavity upon dimerization. Host-guest studies are being pursued.

New macrocycle precursors need to be designed to enhance the usefulness of Schiff base macrocycles as templates for the formation of metallocavitands. Effects on the cavity dimensions, solubility, and desired ligand-metal coordination should all be considered in the design process. Larger diameter macrocycles seem to favor deeper cavities but drastic expansion of the cycle's diameter may inhibit metal cluster formation. Lastly, development of macrocycles with latent functionality that may be exploited after metallocavitand formation would provide more opportunity for supramolecular applications.

An ever-increasing demand for "smart" materials, those that recognize and react to external stimuli, has made organic cavitands the focal point of many scientists' research efforts. The marriage of multiple metal centers and a size-specific cavity, epitomized by metallocavitands, holds a wealth of opportunity to explore molecular recognition phenomena.

Schiff base macrocycle templates, among other systems, are beginning to provide the synthetic reliability necessary for metallocavitands to be embraced by the scientific community, pushing the frontier of supramolecular chemistry.

ACKNOWLEDGEMENTS

The authors are grateful to NSERC and UBC for funding our research on metallocavitands, and to the talented students who have worked on aspects of this chemistry, particularly Amanda Gallant and Jonathan Chong. We also thank Francesco Lelj for helpful discussions and computational studies.

REFERENCES

1. (a) Biros, S. M. and J. Rebek, Jr., 2007. *Chem. Soc. Rev.*, **36**, 93–104. (b) Makha, M., A. Purich, C. L. Raston, and A. N. Sobolev, 2006. *Eur. J. Inorg. Chem.*, 507–517. (c) Dalgarno, S. J., J. L. Atwood, and C. L. Raston, 2006. *Chem. Commun.*, 4567–4574. (d) Müller, A., H. Reuter, and S. Dillinger, 1995. *Angew. Chem. Int. Ed.*, **34**, 2328–2361.
2. Moran, J. R., S. Karbach, and D. J. Cram, 1982. *J. Am. Chem. Soc.*, **104**, 5826–5828.
3. Recent examples: (a) Daly, S. M., M. Grassi, D. K. Shenoy, F. Ugozzoli, and E. Dalcanale, 2007. *J. Mater. Chem.*, **17**, 1809–1818. (b) Ballester, P. and M. A. Sarmentero, 2006. *Org. Lett.*, **8**, 3477–3480. (c) Kim, S. K., B.-S. Moon, J. H. Park, Y. I. Seo, H. S. Koh, Y. J. Yoon, K. D. Lee, and J. Yoon, 2005. *Tetrahedron Lett.*, **46**, 6617–6620. (d) Pinalli, R., M. Suman, and E. Dalcanale, 2004. *Eur. J. Org. Chem.*, 451–462.
4. (a) Zhang, H. and D. M. Rudkevich, 2007. *Chem. Commun.*, 4893–4894. (b) Boerrigter, H., T. Tomasberger, W. Verboom, and D. N. Reinhoudt, 1999. *Eur. J. Org. Chem.*, 665–674.
5. Recent examples: (a) Hooley, R. J. and J. Rebek, Jr., 2007. *Org. Biomol. Chem.*, **5**, 3631–3636. (b) Butterfield, S. M. and J. Rebek, Jr., 2007. *Chem. Commun.*, 1605–1607. (c) Zelder, F. H. and J. Rebek, Jr., 2006. *Chem. Commun.*, 753–754. (d) Kang, J. and J. Rebek, Jr., 1997. *Nature*, **385**, 50–52.
6. Rebek, J., Jr. 2007. *Chem. Commun.*, 2777–2789.
7. Recent examples: (a) Poorters, L., D. Armspach, D. Matt, L. Toupet, and P. G. Jones, 2007. *Angew. Chem. Int. Ed.*, **46**, 2663–2665. (b) Power, N. P., S. J. Dalgarno, and J. L. Atwood, 2007. *Angew. Chem. Int. Ed.*, **46**, 8601–8604. (c) Yamanaka, M., Y. Yamada, Y. Sei, K. Yamaguchi, and K. Kobayashi, 2006. *J. Am. Chem. Soc.*, **128**, 1531–1539. (d) Menozzi, E. and J. Rebek,

Jr., 2005. *Chem. Commun.*, 5530–5532. (e) Richeter, S. and J. Rebek, Jr., 2004. *J. Am. Chem. Soc.*, **126**, 16280–16281. (f) Kersting, B, 2004. *Z. Anorg. Allg. Chem.*, **630**, 765–780.

8. (a) Botana, E., E. Da Silva, J. Benet-Buchholz, P. Ballester, and J. de Mendoza, 2007. *Angew. Chem. Int. Ed.*, **46**, 198–201. (b) Maekawa, M., H. Konaka, T. Minematsu, T. Kuroda-Sowa, M. Munakata, and S. Kitagawa, 2007. *Chem. Commun.*, 5179–5181. (c) Sigouin, O., C. N. Garon, G. Delaunais, X. Yin, T. K. Woo, A. Decken, and F.-G. Fontaine, 2007. *Angew. Chem. Int. Ed.*, **46**, 4979–4982. (d) Jones, L. F., C. A. Kilner, M. P. de Miranda, J. Wolowska, and M. A. Halcrow, 2007. *Angew. Chem. Int. Ed.*, **46**, 4073–4076. (e) Yu, S.-Y., T. Kusukawa, K. Biradha, and M. Fujita, 2000. *J. Am. Chem. Soc.*, **122**, 2665–2666.
9. The notation [X+Y] is commonly used in the Schiff base macrocycle literature to indicate the condensation of X diamines with Y dialdehydes. In the case of oligomers, X and Y need not be equal. *In macrocycles*, however, X = Y.
10. Pilkington, N. H. and R. Robson, 1970. *Aust. J. Chem.*, **23**, 2225–2236.
11. (a) Givaja, G., M. Volpe, J. W. Leeland, M. A. Edwards, T. K. Young, S. B. Darby, S. D. Reid, A. J. Blake, C. Wilson, J. Wolowska, E. J. L. McInnes, M. Schöder, and J. B. Love, 2007. *Chem. Eur. J.*, **13**, 3707–3723. (b) Arnold, P. L., D. Patel, A. J. Blake, C. Wilson, and J. B. Love, 2006. *J. Am. Chem. Soc.*, **128**, 9610–9611. (c) Veauthier, J. M., E. Tomat, V. M. Lynch, J. L. Sessler, U. Mirsaidov, and J. T. Markert, 2005. *Inorg. Chem.*, **44**, 6736–6743. (d) Veauthier, J. M., W.-S. Cho, V. M. Lynch, and J. L. Sessler, 2004. *Inorg. Chem.*, **43**, 1220–1228. (e) Arnold, P. L., A. J. Blake, C. Wilson, and J. B. Love, 2004. *Inorg. Chem.*, **43**, 8206–8208. (f) Givaja, G., A. J. Blake, C. Wilson, M. Schröder, and J. B. Love, 2003. *Chem. Commun.*, 2508–2509.
12. Givaja, G., M. Volpe, M. A. Edwards, A. J. Blake, C. Wilson, M. Schröder, and J. B. Love, 2007. *Angew. Chem. Int. Ed.*, **46**, 584, 586.
13. Tomat, E., L. Cuesta, V. M. Lynch, and J. L. Sessler, 2007. *Inorg. Chem.*, **46**, 6224–6226.
14. Barreira Fontecha, J., S. Goetz, and V. McKee, 2002. *Angew. Chem. Int. Ed.*, **41**, 4553–4556.
15. Barreira Fontecha, J., S. Goetz, and V. McKee, 2005. *Dalton Trans.*, 923–929.
16. Weitzer, M. and S. Brooker, 2005. *Dalton. Trans.*, 2448–2454.
17. (a) Tandon, S. S., L. K. Thompson, J. N. Bridson, and C. Benelli, 1995. *Inorg. Chem.*, **34**, 5507–5515. (b) Tandon, S. S., L. K. Thompson, and J. N. Bridson, 1992. *J. Chem. Soc., Chem. Commun.*, 911–913.
18. Tandon, S. S., S. D. Bunge, and L. K. Thompson, 2007. *Chem. Commun.*, 798–800.

19. Huck, W. T. S., F. C. J. M. van Veggel, and D. N. Reinhoudt, 1995. *Recl. Trav. Chim. Pays-Bas.*, **114**, 273–276.
20. Akine, S., T. Taniguchi, and T. Nabeshima, 2001. *Tetrahedron Lett.*, **42**, 8861–8864.
21. Gallant, A. J., J. K.-H. Hui, F. E. Zahariev, Y. A. Wang, and M. J. MacLachlan, 2005. *J. Org. Chem.*, **70**, 7936–7946.
22. Gallant, A. J. and M. J. MacLachlan, 2003. *Angew. Chem. Int. Ed.*, **42**, 5307–5310.
23. Gallant, A. J., J. H. Chong, and M. J. MacLachlan, 2006. *Inorg. Chem.*, **45**, 5248–5250.
24. (a) Nabeshima, T., H. Miyazaki, A. Iwasaki, S. Akine, T. Saiki, and C. Ikeda, 2007. *Tetrahedron*, **63**, 3328–3333. (b) Nabeshima, T., H. Miyazaki, A. Iwasaki, S. Akine, T. Saiki, C. Ikeda, and S. Sato, 2006. *Chem. Lett.*, **35**, 1070–1071.
25. Frischmann, P. D., A. J. Gallant, J. H. Chong, and M. J. MacLachlan, 2008. *Inorg. Chem.*, **47**, 101–112.
26. Koyama, H. and Y. Saito, 1954. *Bull. Chem. Soc. Jpn.*, **27**, 112–114.
27. (a) Jaitner, P., C. Rieker, and K. Wurst, 1997. *Chem. Commun.*, 1245. (b) Cotton, F. A., L. M. Daniels, L. R. Falvello, J. H. Matonic, C. A. Murillo, X. Wang, and H. Zhou, 1997. *Inorg. Chim. Acta.*, 91–102.
28. Frischmann, P. D. and M. J. MacLachlan, 2007. *Chem. Commun.*, 4480–4482.
29. Horman, I. and B. Dreux, 1984. *Helv. Chim. Acta.*, **67**, 754–764.
30. (a) Kang, J. and J. Rebek, Jr., 1996. *Nature*, **382**, 239–241. (b) Cram, D. J., H. J. Choi, J. A. Bryant, and C. B. Knobler, 1992. *J. Am. Chem. Soc.*, **114**, 7748–7765.

Peter Frischmann completed a BSc at Idaho State University with Dr. Josh Pak in 2005. He is currently a PhD candidate with Dr. Mark MacLachlan at the University of British Columbia. His research is focused on the design and synthesis of new metal-containing supramolecular materials.

Mark J. MacLachlan is an associate professor of chemistry at the University of British Columbia. Previously, he completed his PhD at the University of Toronto with Ian Manners and Geoff Ozin, and worked as an NSERC Post-Doctoral Fellow with Timothy Swager at MIT. His research interests now include supramolecular coordination chemistry and nanostructured materials.